scientific reports

Check for updates

OPEN

Loss of O^6-methylguanine DNA methyltransferase (MGMT) in macrophages alters responses to TLR3 stimulation and enhances DNA double-strand breaks and mitophagy

Md Fazlul Haque[1,2], Salisa Benjaskulluecha[1,3], Atsadang Boonmee[1,4], Pornrat Kongkavitoon[1,3], Benjawan Wongprom[1,3], Thitiporn Pattarakankul[1,5], Rahat Ongratanaphol[6], Kittitach Sri-ngern-ngam[1,3], Chitsuda Pongma[1,7], Benjawan Saechue[8], Patipark Kueanjinda[9], Takashi Kobayashi[10], Asada Leelahavanichkul[9] & Tanapat Palaga[1,3]✉

O^6-methylguanine-DNA methyltransferase (MGMT) is a DNA damage repair enzyme. The roles of this enzyme in immune cells remain unclear. In this study, we explored the roles of MGMT in bone marrow-derived murine macrophages (BMMs) via the use of MGMT knockout (KO) mice. Loss of MGMT altered the response to TLR3 agonists (poly (I:C)), such as dampening the production of TNFα and IL-6. Increased DNA double-strand breaks (DSBs) were observed in MGMT-KO macrophages but did not result in increased cell death. MGMT localized to both nuclei and mitochondria at increasing levels during poly (I:C) stimulation. MGMT deficiency increased the production of mitochondrial reactive oxygen species (mtROS), which was correlated with increased mitophagy. The underlying mechanism involves mediation through activation of the AMPKα pathway. Taken together, our findings reveal the roles of MGMT in macrophages in regulating the response to TLR3, which links DSBs to mtROS and mitophagy via the AMPKα pathway. These roles may have consequences for the inflammatory response and chronic inflammation.

Keywords MGMT, Macrophages, TLR3, Mitochondria, Autophagy

O^6-methylguanine-DNA methyltransferase (MGMT) is a critical DNA repair enzyme that can be expressed in all types of normal and cancer cells to repair damaged DNA caused by alkylating agents[1,2]. Alkylating agents cause damage to guanine nucleotides of DNA by adding a methyl group at the O^6 site of guanine, resulting in mispairing of guanine with thymine, causing a point mutation. MGMT repairs damaged guanine by transferring the methyl at the O^6 site to its cysteine residues. Just after DNA damage is repaired, MGMT is degraded through proteasomal degradation; therefore, it is called a suicidal enzyme[3]. However, MGMT-mediated DNA damage

[1]Department of Microbiology, Faculty of Science, Chulalongkorn University, Bangkok 10330, Thailand. [2]Department of Zoology, Faculty of Biological Sciences, University of Rajshahi, Rajshahi 6205, Bangladesh. [3]Center of Excellence in Immunology and Immune-Mediated Diseases, Chulalongkorn University, Bangkok 10330, Thailand. [4]Department of Microbiology, Faculty of Medicine Siriraj Hospital, Mahidol University, Bangkok 10700, Thailand. [5]Center of Excellence in Advanced Materials and Biointerfaces, Chulalongkorn University, Bangkok 10330, Thailand. [6]Program of Bachelor of Science in Applied Chemistry (BSAC), Faculty of Science, Chulalongkorn University, Bangkok 10330, Thailand. [7]Graduate Program in Biotechnology, Faculty of Science, Chulalongkorn University, Bangkok 10330, Thailand. [8]One Health Research Unit, Faculty of Veterinary Science, Mahasarakham University, Mahasarakham 44000, Thailand. [9]Department of Microbiology, Faculty of Medicine, Chulalongkorn University, Bangkok 10330, Thailand. [10]Department of Infectious Disease Control, Faculty of Medicine, Research Center for GLOBAL and LOCAL Infectious Diseases, Oita University, Oita 879-5593, Japan. ✉email: tanapat.p@chula.ac.th

repair has opposite effects on cancer prevention and cancer treatment[2]. In healthy cells, MGMT repairs spontaneous DNA damage to protect cells from the deleterious effects of mutation, whereas in cancer cells, MGMT repairs chemotherapy-induced damaged DNA to protect cancer cells from death[2]. Thus, MGMT is an important protein in the context of cancer chemotherapy resistance, especially resistance to alkylating agents such as temozolomide, which are used against glioblastoma[4].

Recently, several studies have reported that immune cells, mainly macrophages present in the tumor microenvironment, play a key role in the outcome of chemotherapy treatment[5]. Furthermore, various genotoxic conditions, such as reactive oxygen and nitrogen intermediates, can stimulate the activation of the MGMT protein to repair damaged DNA in macrophages during inflammation[6]. DNA damage in immune cells has also been reported to play a vital role in modulating immune response checkpoints and subsequent diseases[7]. Interestingly, macrophages have been shown to play important roles in regulating the systemic response to DNA damage via a nonautonomous cell mechanism[8]. Until recently, the role(s) of MGMT, if any, in immune cells were largely undocumented. We recently revealed the involvement of MGMT in beta-glucan-induced trained immunity in macrophages[9]. A detailed study on trained immunity revealed that MGMT in macrophages promotes innate immune memory, partially via the FXR and AMPK axes[10]. However, how MGMT, as a DNA damage repair enzyme, regulates the effector functions of innate immune cells is still inadequately understood.

Among the TLR protein family, which forms a large family of pattern recognition receptors (PRRs), TLR3 plays an important role in antiviral innate immune responses by mediating the induction of type I interferons (IFNs) and other proinflammatory cytokines and chemokines. Among the agonists, TLR3 recognizes polyinosinic: polycytidylic acid (poly(I:C)), a mimic of viral dsRNA, dsRNA viruses and ssRNA viruses[11]. TLR3 signaling depends on TRIF and TRAF family member-associated NF-κB activator (TANK)-binding kinase 1 (TBK1). This signaling pathway ultimately activates transcription factors, namely, IRF3/7, NF-κB, and AP-1. TLR3 also activates PI3K and MAPKs that culminate in type I IFN production[12].

In this study, we aimed to investigate the impacts of MGMT deficiency on the innate immune characteristics of macrophages. We observed a link between TLR activation, DNA double-strand breaks (DSBs) and mitochondrial stress via MGMT. The findings presented here indicate that MGMT may play a crucial role in regulating how macrophages cope with mitochondrial stress during stimulation by pathogen-associated molecular patterns.

Results

MGMT deficiency affects the macrophage response to stimulation by a TLR3 agonist

Because MGMT plays a key role in the DNA repair of methylated guanine lesions as a result of exposure to alkylating agents, we investigated how the loss of MGMT influences the susceptibility of bone marrow-derived macrophages (BMMs) to the alkylating agents, streptozotocin (STZ) and N-nitroso-N-methylurea (NMU). Deficiency in MGMT was confirmed in BMMs from KO mice, as shown in Supplementary Fig. S1A. Upon treatment with alkylating agents, both WT and MGMT KO BMMs showed comparable sensitivity to NMU in a dose-dependent manner, whereas no discernible loss in cell viability was observed in response to STZ (Supplementary Fig. S1B). Therefore, DNA repair in lesions upon exposure of macrophages to alkylating agents may rely on mechanisms other than MGMT. Thus, we explored the roles of MGMT in regulating the effector functions of macrophages other than the function of DNA repair.

To investigate how the loss of MGMT affects the response of macrophages to stimuli, we investigated their responses to classical M1 (LPS, IFN-γ) and M2 (IL-4) stimulation. Stimulation with LPS or LPS/IFNγ induced the expression of genes encoding proinflammatory cytokines (*TNFA*, *IL6* and *IL1B*) and the production of TNFα and IL-6 in the MGMT-KO BMMs at comparable levels to those in the WT BMMs (Supplementary Fig. S2A, B). The levels of nitric oxide (NO) and surface markers (CD40 and MHC class II) were also similar (Supplementary Fig. S2C–F). Next, IL-4 was used to polarize BMMs toward the M2 phenotype. As shown in Supplementary Fig. S3A–C, both WT and MGMT-KO BMMs expressed representative M2 genes (*IL10*, *Fizz1* and *ArgI*) at comparable levels. The surface expression of CD206 was also similar (Supplementary Fig. S3D–G). Taken together, these findings indicate that MGMT is dispensable for classical M1 or M2 polarization in BMMs.

We next stimulated BMMs with the TLR3 agonist poly (I:C), a strong type I IFN inducer, and measured their responses. The expression of proinflammatory cytokine genes (*TNFA*, *IL6*, *IL1B* and *IL12p40*) was significantly lower in the MGMT-KO BMMs than in the WT BMMs (Fig. 1A). The levels of secreted TNFα and IL-6 were also lower in the MGMT-KO BMMs than in the control BMM (Fig. 1B). The level of *IFNB* mRNA was lower in the MGMT-KO BMMs than in the control BMM at earlier time points (2 h) but was not different at later time points (6 h) (Fig. 1C).

In contrast to the dampened proinflammatory response against poly (I:C) stimulation, the expression of *IL10* and *iNOS* and the production of IL-10 and NO were significantly greater in the MGMT-KO BMMs (Supplementary Fig. S4A, B). Taken together, these results revealed that MGMT deficiency in macrophages altered poly (I:C)-induced inflammatory responses by dampening the expression of proinflammatory cytokines, as well as by potentiating the expression of NO and the anti-inflammatory cytokine IL-10.

MGMT deficiency enhances the accumulation of DNA double-strand breaks (DSBs) in macrophages

Because MGMT is responsible for DNA damage repair, loss of MGMT may result in DNA damage in the form of DSBs. γ-H2AX foci formation is a well-known marker of DSBs[13]. Therefore, an immunofluorescence assay for the quantification of γ-H2AX foci formation in BMMs was performed to investigate the effect of MGMT deficiency on the DNA damage response under unstimulated and poly (I:C)-stimulated conditions. The results revealed that the number of γ-H2AX foci per nucleus was significantly greater in the MGMT-KO macrophages than in the WT macrophages under unstimulated conditions (Fig. 2A,B). This result indicated that, compared with WT macrophages, MGMT KO macrophages were more prone to DSBs. In addition, γ-H2AX foci

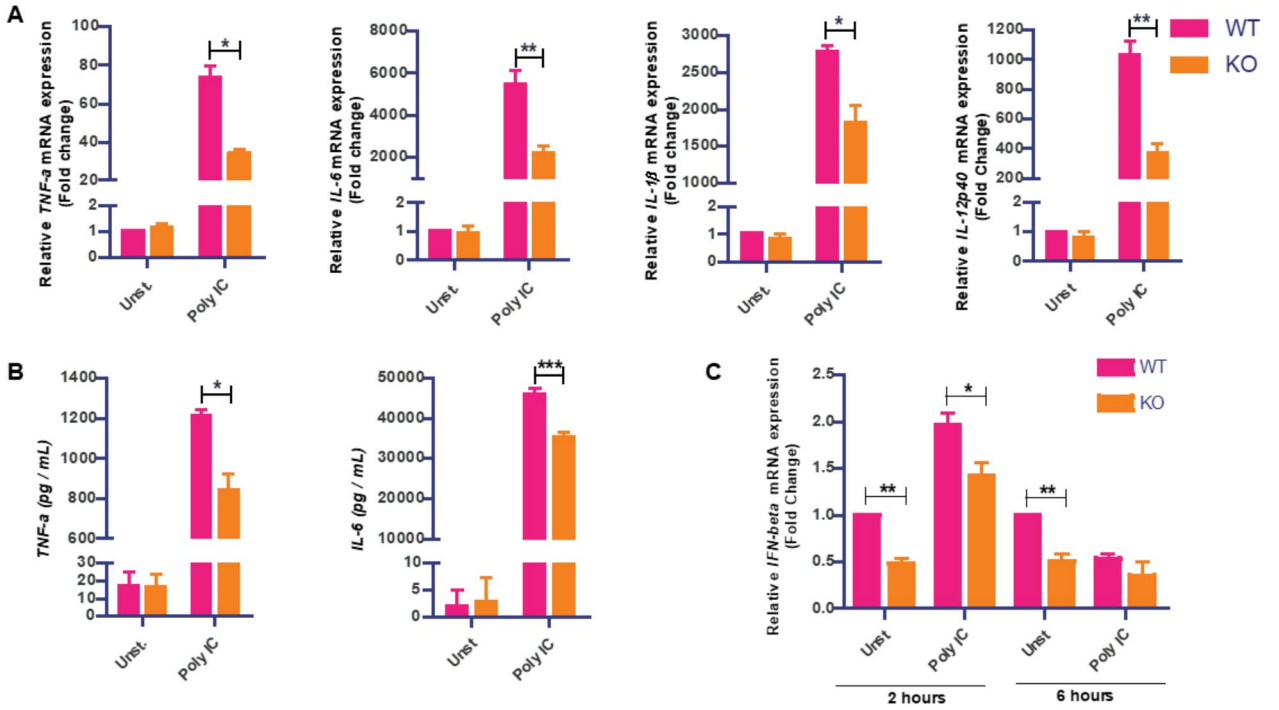

Fig. 1. Altered responses to TLR3 stimulation in MGMT KO BMMs. WT and MGMT-KO BMMs were treated with poly (I:C) (20 μg/ml) and incubated for 6–24 h. (**A**) After 6 h, the cells were collected and processed for RNA extraction, cDNA conversion and qPCR of *TNFA*, *IL6*, *IL12p40* and *IL1B* mRNAs. (**B**) After 24 h, the culture supernatant was collected and processed for ELISA for TNFα and IL-6. The data are presented as the means ± SEMs from at least three independent experiments. $^{***}P < 0.001$, $^{**}P < 0.01$, $^{*}P < 0.05$. (**C**) Cells were treated as described above for 2 and 6 h, and total RNA was subjected to qPCR to determine the relative expression of *IFNB*. The data are presented as the means ± SEMs from three independent experiments. $^{**}P < 0.01$, $^{*}P < 0.05$.

formation increased substantially when WT and MGMT KO macrophages were stimulated with poly (I:C) (Fig. 2B), demonstrating the role of poly (I:C) in exacerbating DNA damage in macrophages and that MGMT is responsible for suppressing DSBs under these conditions.

DSBs in nuclei typically lead to the accumulation of DNA damage and ultimately to cell death. Therefore, we measured cell viability using two approaches: an intracellular ATP assay and an MTT assay. The intracellular ATP assay consistently revealed lower luminescence signals in the MGMT-KO macrophages with or without poly (I:C) stimulation (Fig. 2C). In contrast, the MTT assay revealed comparable cell viability between WT and MGMT-KO cells under all conditions, except for a slight reduction only upon poly (I:C) stimulation in the MGMT-KO BMMs (Fig. 2D). Therefore, in the resting stage, the loss of MGMT may result in lower intracellular ATP conditions while preserving cell viability, as measured by mitochondrial reductase activity with the MTT assay.

MGMT localizes to the nucleus and mitochondria in macrophages

We next examined the cellular localization of MGMT puncta with or without poly (I:C) stimulation. Surprisingly, we found that MGMT puncta were present not only in the nucleus but also in the cytoplasm of BMMs under both unstimulated and poly (I:C)-stimulated conditions (Fig. 3A,B). Moreover, the numbers of MGMT puncta in both the nucleus and cytoplasm of macrophages were significantly greater after stimulation with poly (I:C) than in unstimulated conditions (Fig. 3A, B). To pinpoint the cytoplasmic location of MGMT, the mitochondrial marker HSP60 was used for costaining. The colocalization of MGMT and HSP60 increased significantly following poly (I:C) stimulation, indicating that MGMT colocalized with mitochondria (Fig. 3C).

To confirm this unexpected finding, we performed cellular fractionation and Western blotting and observed that MGMT was detectable in both the nuclear and cytoplasmic fractions, with more intense signals after poly (I:C) stimulation (Fig. 3D and Supplementary Fig. S5). Thus, the presence of MGMT puncta in both the cytoplasm (mitochondria) and nucleus indicated that MGMT potentially functions not only in the nucleus but also in the cytoplasm in macrophages. Upon poly (I:C) stimulation, MGMT accumulates in mitochondria, indicating a key function in response to stimulation. It has been previously reported that MGMT is present in the cytoplasm to repair mitochondrial DNA damage caused by alkylating agents in the lymphoblast cell line K-562 [14], but similar evidence for macrophages has not been presented until now.

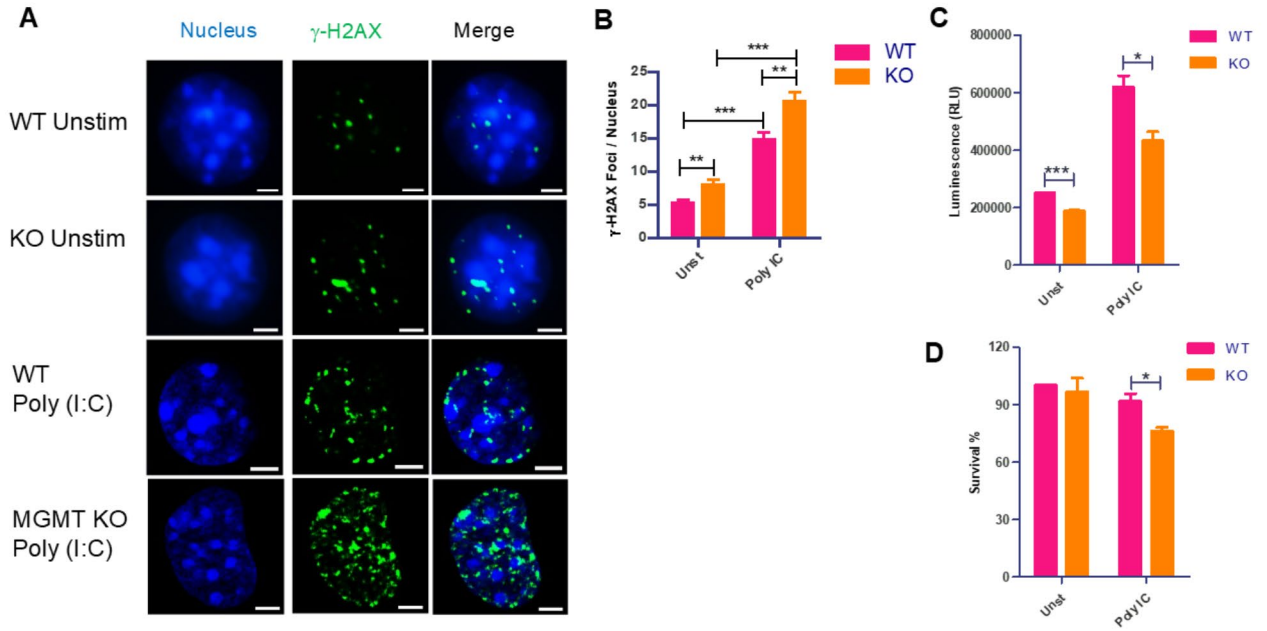

Fig. 2. Increased accumulation of DSBs in the MGMT-KO BMMs. (**A**,**B**) WT and MGMT KO BMMs were seeded on chamber slides, stimulated with poly (I:C) (20 μg/ml) and incubated further for 24 h. The cells were then fixed and stained for γ-H2AX and nuclear dye. The cells were processed for confocal microscopy analysis of the DNA damage marker γ-H2AX. The data are presented as the means ± SEMs from three independent experiments. At least 50 nuclei per condition per independent experiment were quantified. Scale bar 2 μM. $^{***}P < 0.001$, $^{**}P < 0.01$. (**C**,**D**) WT and MGMT KO bone marrow-derived macrophages were treated with poly (I:C) (20 μg/ml) and incubated for 24 h. After incubation, the cells were processed for ATP assays to measure intracellular ATP production or for MTT assays to calculate the cell survival rate. The data are presented as the means ± SEMs from at least three independent experiments. $^{**}P < 0.01$ and $^{*}P < 0.05$.

MGMT deficiency increases ROS and mtROS production in macrophages

Microbial stimulation of macrophages is linked to changes in mitochondrial metabolism, including changes in the mitochondrial membrane potential and the release of mitochondrial reactive oxygen species (mtROS) and mitochondrial DNA (mtDNA)[15]. Furthermore, several studies have reported that excess ROS generated by damaged mitochondria can trigger autophagy[16–18]. Therefore, we hypothesized that MGMT KO macrophages may be under mitochondrial stress due to excess ROS production. Using DCFH-DA fluorescence dye to detect ROS, we observed that the fluorescence intensity of the ROS was significantly greater in the MGMT-KO BMMs than in the WT BMMs under all the experimental conditions (Fig. 4A). Poly (I:C) treatment further increased ROS production (Fig. 4A). Moreover, the fluorescence intensity of ROS further increased in BMMs when autophagic flux was inhibited by treatment with bafilomycin A1 (Fig. 4A), indicating a link between autophagy and the clearance of excess ROS.

ROS in macrophages can be generated by damaged mitochondria as well as from other organelle sources[19]. Therefore, we used Mitochondrial Superoxide (MitoSOX), which is specific for mitochondria-specific ROS (mtROS), in BMMs with or without bafilomycin A1 treatment to investigate whether the ROS in the MGMT-KO BMMs were derived from mitochondria. The results revealed that the MGMT KO BMMs stained brightly for MitoSOX, which colocalized well with HSP60 (Fig. 4B). The corrected total cell fluorescence (CTCF) of MitoSOX was significantly greater in the MGMT-KO BMMs than in the WT BMMs and was further markedly increased by treatment with bafilomycin A1 (Fig. 4C). Our data thus far strongly indicate that MGMT localizes to mitochondria and regulates ROS production. In the absence of MGMT with poly (I:C) treatment, mtROS increases, a mechanism that is required for autophagy in controlling mtROS levels.

MGMT deficiency enhances autophagy in the BMM

Several studies have reported that ROS, mainly mtROS, can induce autophagy in macrophages and other cell types via the AMPK and mTOR axes[20–23]. Hence, we monitored autophagy in the BMM via immunofluorescence staining and Western blotting. In this study, autophagic flux was inhibited by bafilomycin A1 treatment. The increased lipidation of LC3B in the MGMT KO BMMs was supported by the analysis of IF images of LC3B puncta, which revealed that the number of LC3B puncta per cell was markedly greater in the MGMT KO BMMs than in the WT BMMs under all the studied conditions (Fig. 5A,B). The Western blot results also revealed that the band density of the lipidated form of LC3B, called LC3-ii, a marker protein of the autophagosome and autolysosome membrane, was significantly greater in MGMT-KO macrophages than in WT macrophages with or without poly (I:C) treatment when autophagic flux was inhibited with bafilomycin A1 (Fig. 5C and

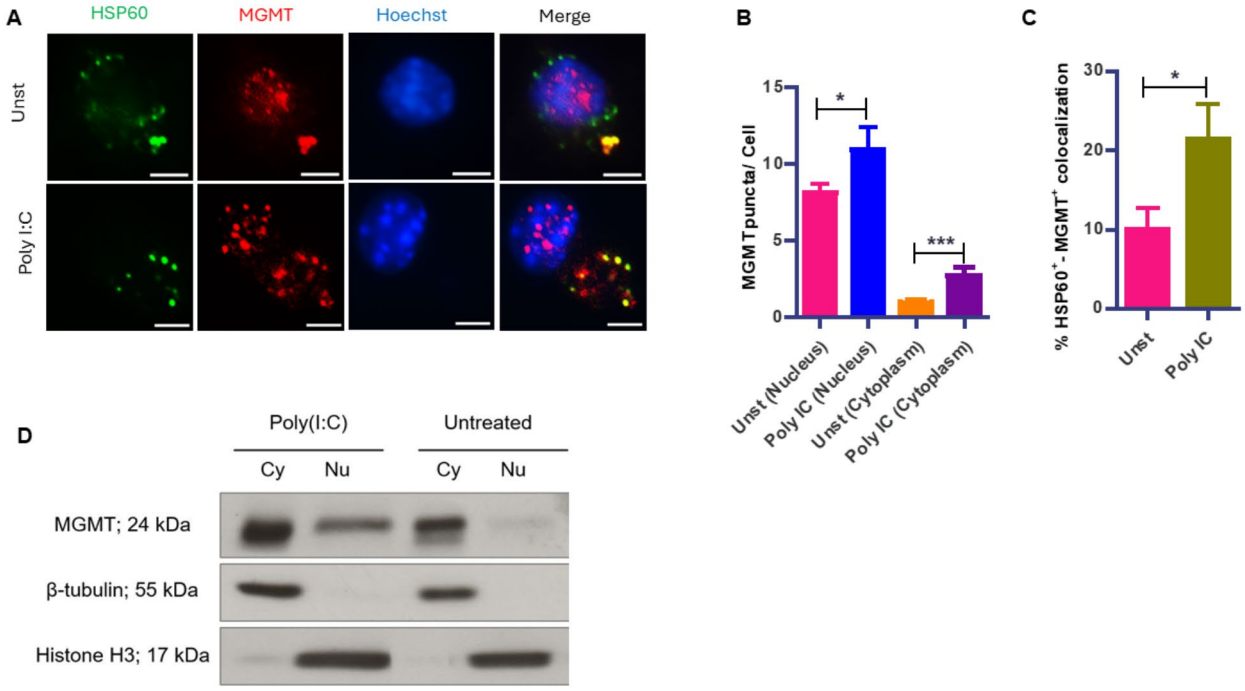

Fig. 3. Poly (I:C) stimulation increases the MGMT level in the nuclei and mitochondria of BMMs. (**A**) WT BMMs were stimulated with poly (I:C) (20 µg/ml) and incubated for 24 h. The cells were then fixed and stained for MGMT, HSP60 (a mitochondrial marker) and the nucleus. The cells were processed for confocal microscopy analysis. Scale bar = 5 µM. (**B**) MGMT puncta were quantified in at least 50 cells per condition per independent experiment. The data are presented as the means ± SEMs from three independent experiments. $^{*}P < 0.05$. (**C**) Colocalization of MGMT puncta and Hsp60 quantified in at least 50 cells per condition per independent experiment. The co-localization percentage was calculated using the double positive foci/ MGMT + foci. $^{*}P < 0.05$. (**D**) BMMs from WT mice were stimulated with poly (I:C) as described above, and cytoplasmic and nuclear fractionation was performed. Lysates were subjected to Western blotting to detect MGMT, β-tubulin and histone proteins.

Supplementary Fig. 6). These results strongly indicate that the loss of MGMT in macrophages spontaneously triggers autophagy.

MGMT deficiency increases mitophagy in macrophages

Clearing damaged mitochondria by autophagy, termed mitophagy, is an essential mechanism for addressing damaged organelles[24,25]. However, the link between MGMT and mitophagy has not yet been studied. On the basis of our findings that MGMT deficiency results in increased mtROS and autophagy and the localization of MGMT to mitochondria, we investigated whether mtROS potentially damages mitochondria, which need mitophagy for their clearance, in the MGMT-KO BMMs and in the WT BMMs. To track mitophagy in macrophages, we stained mitochondria, autophagosomes and autophagolysosomes with HSP60, LC3B and LysoTracker™, respectively. We found that under unstimulated conditions, the colocalization of HSP60 with LC3B or LysoTracker™ was significantly greater in the MGMT-KO macrophages than in the WT macrophages (Fig. 6A,B). The percentage of colocalization of HSP-60 with LC3B was further increased in the MGMT-KO cells but not in the WT macrophages after treatment with bafilomycin A1 (Fig. 6A,B), indicating that the MGMT-KO BMMs accumulated more mitochondria containing autophagosomes than did the WT macrophages. Similarly, the percentage of colocalization of HSP60 with LysoTracker™ markedly decreased in both MGMT KO and WT macrophages after treatment with bafilomycin A1 (Fig. 6C,D), indicating the inhibition of autophagolysosome biogenesis due to prevention of the fusion of autophagosomes with lysosomes by bafilomycin A1 [26]. Thus, the increased colocalization of mitochondria with autophagosomes and autophagolysosomes in MGMT-KO macrophages and the alteration by an autophagy inhibitor confirmed that MGMT deficiency is actively involved in the induction of mitophagy, potentially to clear damaged mitochondria in macrophages.

Mitophagy is a crucial process for mitochondrial homeostasis[25]. To investigate how excess mitophagy induced by the loss of MGMT affects mitochondrial biomass, mitochondria were stained with MitoTracker™ Green, and the fluorescence intensity was analyzed via flow cytometry and a microplate reader. The mitochondria were also stained with HSP60, and the number of mitochondria per cell was analyzed via confocal microscopy. The results revealed that the fluorescence intensity of MitoTracker™ Green and the number of mitochondria per cell were markedly lower in the MGMT-KO macrophages than in the WT macrophages, which was reversed when mitophagy was inhibited by bafilomycin A1 treatment (Supplementary Fig. S7A–F).

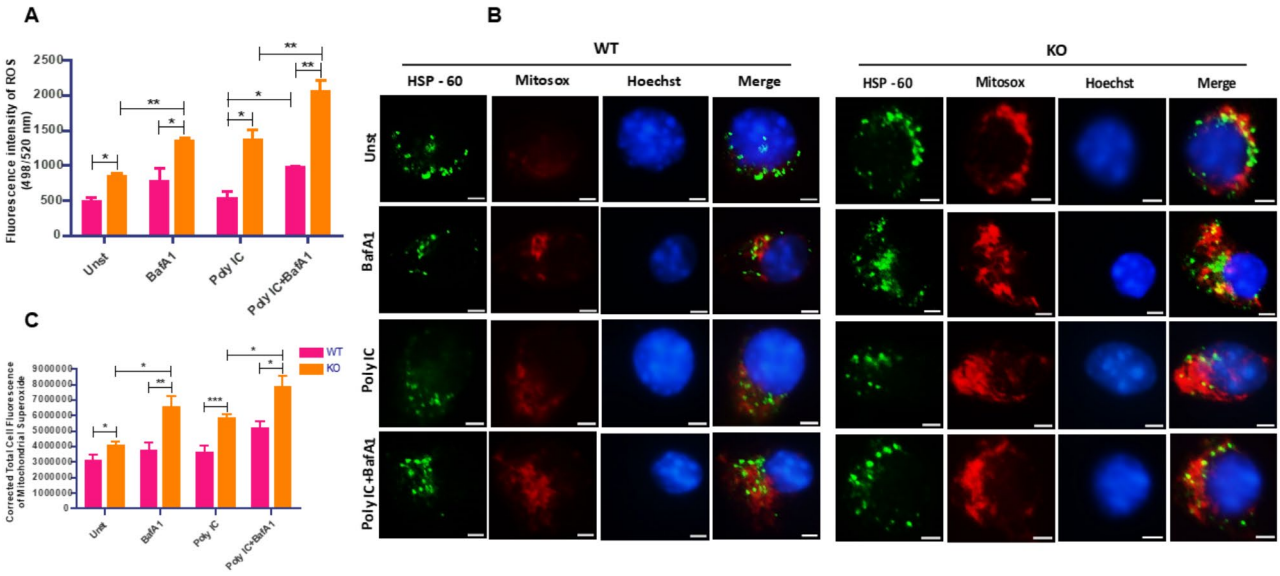

Fig. 4. Loss of MGMT increases ROS and mtROS production in BMMs. (**A**) WT and MGMT-KO BMMs were treated with bafilomycin A1 (500 nM), poly (I:C) (20 μg/ml) or poly (I:C) with bafilomycin A1 and incubated for 24 h. After incubation, the cells were treated with DCFH-DA (10 μM) for 15 min, washed with PBS, and the fluorescence intensity of the ROS was immediately measured at 498/520 nM via a microplate reader. (**B**,**C**) Cells were fixed and stained for HSP60 and nuclei and were subsequently stained with MitoSOX reagent (5 μM) for 10 min. The cells were processed for confocal microscopy analysis. Scale bar = 2 μM. (**C**) Corrected total cell fluorescence (CTCF) of MitoSOX was performed on the basis of the images obtained from (**B**). The data are presented as the means ± SEMs from three independent experiments. $^{***}P < 0.001$, $^{**}P < 0.01$ and $^{*}P < 0.05$.

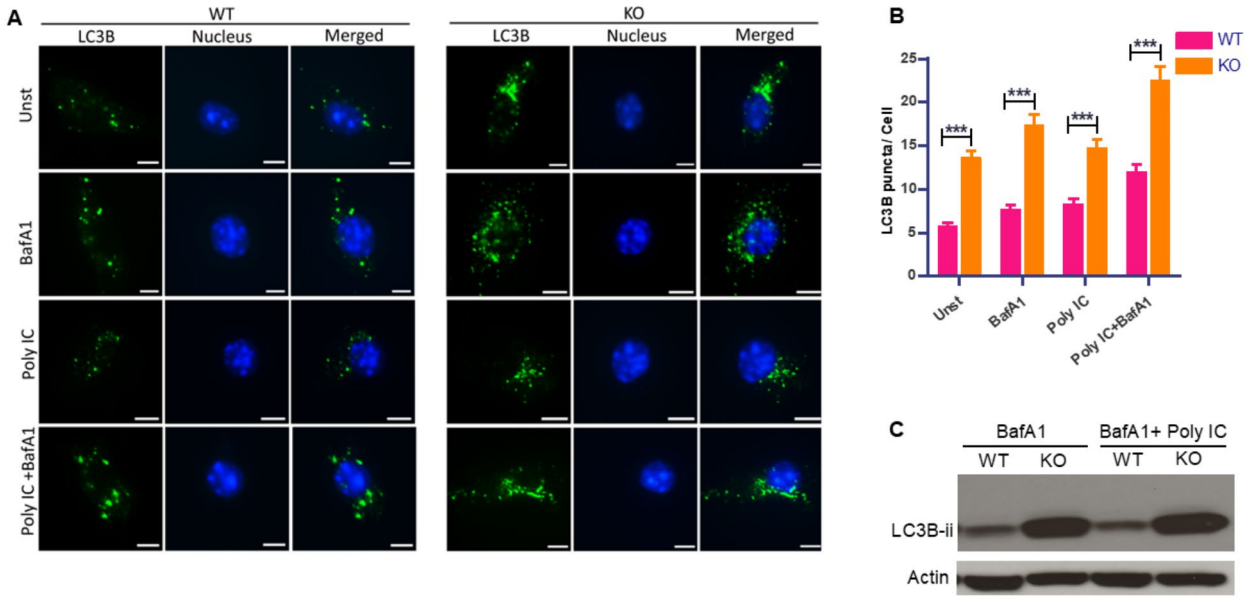

Fig. 5. Loss of MGMT increases autophagy in BMMs. WT and MGMT-KO BMM were pretreated with bafilomycin A1 (500 nM) for 1 h. The cells were stimulated with poly (I:C) (20 μg/ml) and incubated for 24 h. (**A**,**B**) Cells were fixed and stained for LC3B and nuclei. At least 50 cells per condition per independent experiment were quantified for LC3B puncta. The data are presented as the means ± SEMs from three independent experiments. Scale bar = 5 μM. $^{***}P < 0.001$, $^{**}P < 0.01$ (**C**) Cells were treated as indicated, and the cell lysates were processed for Western blotting for LC3Bii.

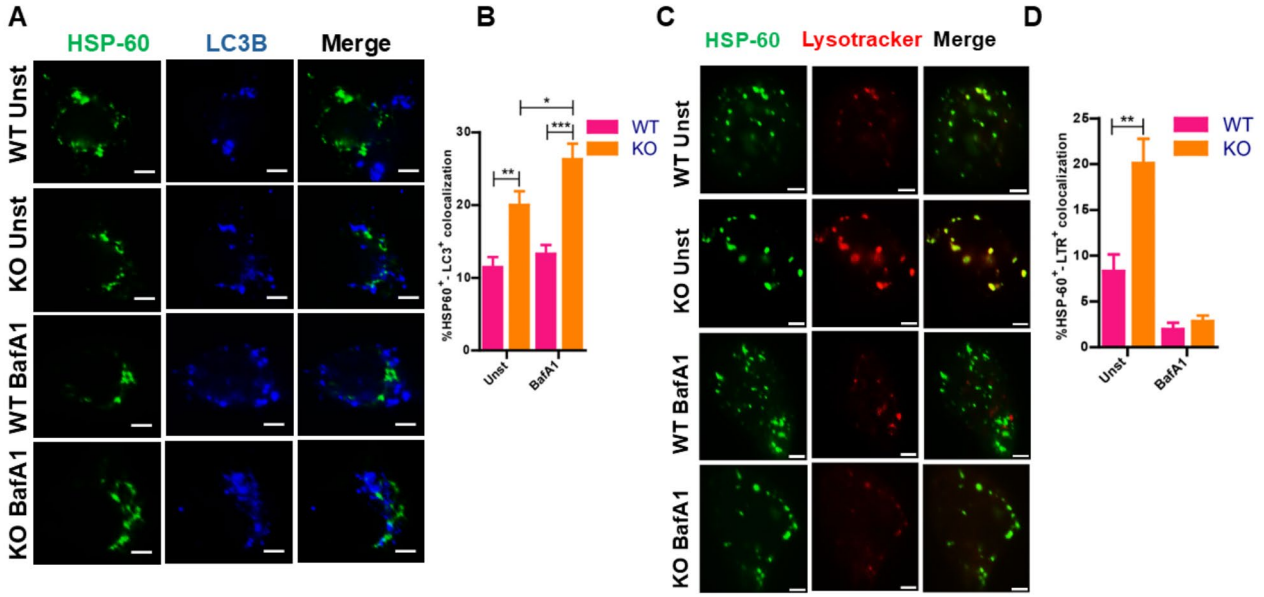

Fig. 6. Loss of MGMT enhances mitophagy in macrophages. (**A**,**B**) WT and MGMT KO BMMs were treated with bafilomycin A1 (500 nM) and incubated for 24 h. The cells were fixed and stained for HSP60 and LC3B and processed for confocal microscopy analysis. The colocalization of HSP60 and LC3B was quantified in at least 50 cells per condition per independent experiment. The data are presented as the means ± SEMs from three independent experiments. Scale bar = 5 µM. $^{***}P < 0.001$, $^{**}P < 0.01$ and $^{*}P < 0.05$. (**C**,**D**) Cells were treated as described above and incubated with LysoTracker Deep Red (100 nM) for 1 h. The cells were then fixed and stained for HSP60 and processed for confocal microscopy analysis. At least 50 cells per condition per independent experiment were quantified for colocalization between lysosomes and HSP60. The data are presented as the means ± SEMs from three independent experiments. $^{***}P < 0.001$, $^{**}P < 0.01$ and $^{*}P < 0.05$.

Activation of AMPKα in the absence of MGMT in macrophages

Next, we detected the phosphorylation of AMPKα and mTOR to verify their involvement in the autophagy induction that was observed at increasing levels in the MGMT-KO BMMs. The Western blot results revealed that the relative density of phosphorylated AMPKα was significantly greater in the MGMT-KO macrophages than in the WT BMMs with or without poly (I:C) stimulation (Fig. 7A). In agreement with this increased AMPKα activation, the relative density of phosphorylated mTOR was lower in the MGMT-KO BMMs than in the WT BMMs (Fig. 7B). To further explore the signaling downstream of TLR3/poly (I:C), the activation of AKT was investigated. As shown in Fig. 7C and Supplementary Fig. S8, the loss of MGMT resulted in increased AKT phosphorylation upon poly (I:C) stimulation. Taken together, the results of the signaling pathway analysis indicated that in the absence of MGMT, mTOR activation was negatively regulated by the ROS-AMPK axis and positively regulated by activated AKT, culminating in decreased mTOR activation and possibly autophagy induction.

In conclusion, we investigated the role of MGMT as a DNA repair enzyme in macrophages in response to stimulation. Loss of MGMT did not directly lead to cell death after stimulation but instead increased the accumulation of DSBs. As a result, the response to TLR3 stimulation was altered, which involved the localization of MGMT to mitochondria and the control of mitochondrial ROS production. Finally, as a result of MGMT loss, the AMPK pathway was activated, which triggers mitophagy.

Discussion

MGMT is a suicidal DNA repair enzyme that removes alkyl groups from position O6 of guanine and is degraded by the ubiquitin proteasome pathway[1,3]. Genomic deletion of MGMT in mice renders fibroblasts more sensitive to the toxic effects of the chemotherapeutic alkylating agents used in cancer treatment. Thus, MGMT plays critical roles in preventing carcinogenesis, while also protecting cancer cells against the therapeutic effects of chemotherapy[2]. In this study, we did not observe differences in the sensitivity of macrophages to the toxicity of alkylating agents in the absence of MGMT. This result may be due to the differentiation and proliferation of macrophages. As terminally differentiated cells, macrophages undergo only minimal cell division, and DNA lesions containing methylated guanines may not immediately cause cells to commit to cell death. Interestingly, DSBs are highly cytotoxic lesions, and cells typically respond to DSBs by either repairing the damage or undergoing cell death if the damage is too severe. Our results showed that DSB accumulated in TLR3-activated BMMs did not undergo cell death at least during the experimental periods of 24 h. Macrophages may show unusual resistance to DSB-induced death by several mechanisms, including enhanced DNA Repair Mechanisms[27], strong pro-survival signaling pathways[28] and cellular senescence[29].

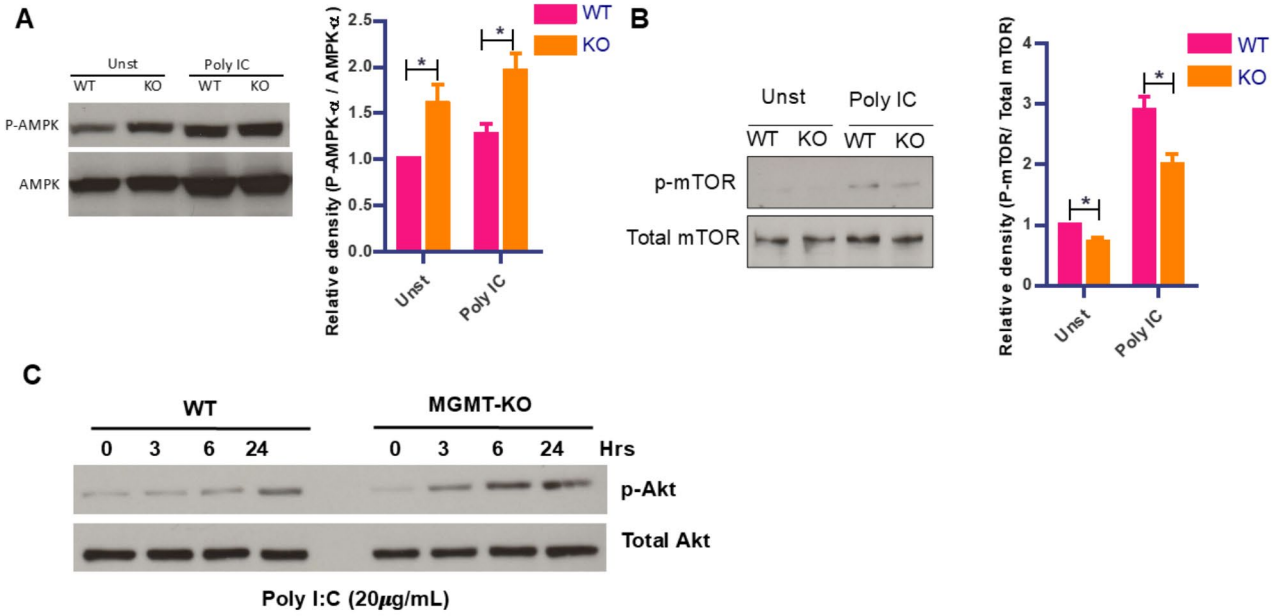

Fig. 7. Activation of the AMPKα, mTOR and AKT pathways in the absence of MGMT in macrophages. (**A**,**B**) WT and MGMT KO BMMs were stimulated with poly (I:C) (20 μg/ml) and incubated for 24 h. The cells were lysed and processed for phospho-AMPKα and total AMPKα or phosphor-mTOR and total mTOR. Normalized relative band densities were obtained and are shown as the means ± SEMs from three independent experiments. $^{*}P < 0.05$. (**C**) WT and MGMT KO BMMs were stimulated with poly (I:C) (20 μg/ml) at the indicated times, and the cell lysates were subjected to Western blotting for phospho-AKT and total AKT.

Activation of pattern recognition receptors, including TLR3, is reported to induce DNA repair genes and increase functional DNA repair, suggesting that presence of DNA damage upon innate immune response[30]. It is speculated that when poly (I:C) stimulates macrophages, it triggers various cellular stress responses that may lead to increased DSBs in the nucleus potentially through DNA damaging mediators such as reactive oxygen intermediates and reactive nitrogen intermediates, such as nitric oxide. It has been reported that ROS causes chronic oxidative DNA damage resulting in DSBs[31]. In this study, activation by TLR3 ligand enhanced DSBs in BMMs and increased DSBs were observed in MGMT-KO BMMs. Accumulation of O^6-methylguanine (O^6-meG) in MGMT-KO macrophages due to lack of repair can lead to DNA double-strand breaks (DSBs) through DNA mismatch repair process[32,33]. Therefore, increased DSBs in MGMT-KO macrophages observed in our study supported a role for MGMT as a DNA repair enzyme.

We recently reported the undocumented roles of MGMT in myeloid cells in the context of trained immunity when MGMT regulates the beta-glucan-induced trained response in macrophages[10]. In this previous report, no difference in response to LPS was observed between WT and MGMT-KO macrophages. In this study, we confirmed the dispensable role of MGMT in macrophage polarization to the M1 (LPS/IFNγ) or M2 (IL-4) phenotype. The transcriptomic analysis of MGMT-KO macrophages revealed a decrease in the IFNα response pathway, which led us to investigate the role of type I IFN-inducing stimuli, such as poly (I:C) (Supplementary Fig. S9). Poly(I:C), which mimics dsRNA and stimulates cells via TLR3, which drives key antiviral responses, including the production of type I IFN, dendritic cell maturation and the activation of natural killer (NK) cells[34]. TLR3 is an RNA sensor that localizes to endosomes and depends on Toll-interleukin-1 receptor (TIR)-domain-containing adaptor-inducing IFN-β (TRIF) for signal transduction [34]. One of the key differences between the TLR4 (LPS) and TLR3 signaling pathways is that TLR4 utilizes both TRIF and MyD88 for signal transduction, whereas TLR3 uses TRIF only [35]. The lack of defects in response to LPS that was observed in poly (I:C) in the MGMT-KO macrophages may be due to differences in signal transduction.

We also found that MGMT deficiency altered poly (I:C)-induced inflammatory responses in macrophages via downregulation of TNF-α, IL-6, IL-1β and IL-12p40 expression but upregulation of iNOS and IL-10 expression. The poly (I:C)-induced upregulation of type I IFNs and proinflammatory cytokines through TLR3-ISRE3/AP1/NF-κB activation has been well documented in other studies[36–38]. The dampened inflammatory response observed in poly (I:C)-activated macrophages could be due to a few possible mechanisms related to DNA damage and immune signaling dysregulation and feedback anti-inflammatory response from increased IL-10 in MGMT-KO macrophages. In signaling studies, AKT phosphorylation was increased in the absence of MGMT, which may explain the increased iNOS and NO production.

The finding that MGMT-KO macrophages produced more mtROS and that MGMT localized to mitochondria led us to focus more on the link between mitochondrial stress and autophagy. In trained immunity, MGMT KO results in decreased glycolytic capacity, which is required for a heightened response, suggesting that MGMT may

be involved in mitochondrial metabolism[10]. Because of the function of MGMT as a DNA repair enzyme, it is intriguing to postulate that MGMT may also function as a mitochondrial DNA (mtDNA) repair factor. mtDNA is more susceptible to damage by DNA-damaging agents than nuclear DNA. Accumulated DNA damage may cause mitochondrial dysfunction and can result in diseases such as neurodegenerative diseases[39]. Direct reversal of O-alkylated and N-alkylated damage caused by DNA alkylating agents may require MGMT. Further studies are needed to explore this intriguing model, which may shed light on how the integrity of mtDNA in macrophages is maintained.

We also found that mtROS generation was significantly greater in MGMT-KO macrophages than in WT macrophages. This event potentially leads to chain reactions, which in turn induce autophagy through the induction of the AMPK-mTOR axis. Because mtROS generated by mitochondria can damage and mutate mtDNA[40], the increase in mtROS in MGMT-KO macrophages could lead to the accumulation of mtDNA damage due to the lack of an MGMT-mediated DNA repair mechanism. Our results are also supported by other studies showing that mitochondrial superoxide can activate AMPK and subsequently suppress mTOR phosphorylation and induce autophagy in macrophages to clear excess ROS from cells[17,22,41].

We observed that the level of intracellular ATP was markedly lower in the MGMT-KO macrophages than in the WT macrophages, which may indicate mitochondrial dysfunction in the MGMT-KO macrophages. Any mutation or damage in mtDNA, which encodes several mitochondrial proteins involved in ATP synthesis, has direct implications for reducing intracellular ATP production[42,43]. Consistent with this model, we detected increased mitophagy in MGMT-KO macrophages, possibly resulting in the clearance of damaged mitochondria, resulting in a reduction in mitochondrial mass compared with that in WT macrophages[44,45].

In conclusion, this study presented evidence that the DNA repair enzyme MGMT plays a critical role in controlling the macrophage response to TLR3/viral infection by modulating mitochondrial stress during the response. We proposed a model where MGMT KO leads to a failure in DNA repair, causing persistent DNA damage and cellular stress. Poly(I:C), by activating innate immune responses, increases ROS production and mitochondrial stress. The combination of these stresses increases mtROS, which further damages mitochondria and triggers the activation of both autophagy and mitophagy to eliminate dysfunctional mitochondria and protect against excessive oxidative damage, partially via AKT/AMPKa axis. This interplay highlights how DNA repair defects, immune activation, and mitochondrial dysfunction can drive compensatory autophagic processes in MGMT KO cells under poly(I:C) treatment.

This insight not only reveals potential roles of MGMT in relation to mitochondrial metabolism but also suggests that it is involved in mtDNA repair and the consequences for the innate immune response against infection. This study used BMMs as a model to study the impact of MGMT deficiency on the macrophage response to stimuli. Whether MGMT plays similar roles in human macrophages remains to be investigated. In addition, macrophages are highly specialized tissue-resident immune cells. Therefore, the role of MGMT in specific niches of macrophages still needs to be further investigated. To determine the role of MGMT in mtDNA repair, a detailed study of macrophages and other cell types is warranted. Finally, the impact of MGMT KO on myeloid cells at the systemic level needs further study in vivo.

Methods

Generation of BMMs

Myeloid-specific MGMT KO mice were generated as previously described[10]. WT and MGMT-KO BMMs were generated from bone marrow cells extracted from the tibias and femurs of WT and MGMT-KO mice. Both WT and MGMT KO bone marrow cells were cultured in BMM medium, which was composed of Dulbecco's modified Eagle's medium (DMEM) (HyClone, USA) supplemented with 10% (v/v) fetal bovine serum (Gibco, USA), 10 mM HEPES (HyClone, USA), 1 mM sodium pyruvate (HyClone, USA), 100 U/ml penicillin, and 0.25 mg/ml streptomycin (DMEM complete media) with 20% L929 culture supernatant and 5% horse serum (HyClone, USA), and fresh media was added on Day 4. After 7 days in culture, the cells were detached with cold PBS and stored at − 80 °C until use. BMMs were confirmed by flow cytometry using the macrophage surface markers F4/80 and CD11b. This study was performed at Chulalongkorn University Laboratory Animal Center (CULAC) with approval protocols No. 2073016 and No. 2173012. All the experiments were performed according to the guidelines issued by the IACUC. The mice were humanely euthanized via carbon dioxide inhalation.

Macrophage stimulation

WT and MGMT KO BMMs were cultured in BMM medium for 24 h at 37 °C and 5% CO_2. The cells were detached with cold PBS, counted, seeded (1×10^6 cells/well/2000 µl in BMM) in a 6-well plate and incubated for 24 h. The BMM media in each well was replaced with 1000 µl of complete DMEM for nonstimulation or 1000 µl of complete DMEM supplemented with *E. coli* LPS (100 ng/ml; L2880, Sigma Aldrich, USA) or LPS + IFNγ (100 ng/ml LPS + 10 ng/ml IFN-γ) for M1 polarization or with IL-4 (100 ng/ml) for M2 polarization. Recombinant cytokines were obtained from BioLegend (USA). For poly (I:C) stimulation, cells were prepared as described above and treated with poly (I:C) (20 µg/ml; InvivoGen, USA). The macrophages were incubated again for the indicated times. Markers of M1 or M2 macrophage polarization were examined via qRT-PCR, ELISA and flow cytometry.

qRT–PCR

WT and MGMT-KO BMMs were treated as indicated, and total RNA was harvested with TRIzol reagent (Invitrogen, USA) and extracted with direct-zol RNA kits (Zymo Research, USA). The quality and concentration of RNA were measured with a NanoDrop™ 2000 spectrophotometer (Thermo Fisher Scientific). At least 200 ng of RNA per sample were converted to cDNA, which was used for quantitative PCR via iQ™ SYBR Green SuperMix (Bio-Rad, USA) according to the manufacturer's instructions. The relative expression of all target

genes (*TNFA*, *IL6*, *IL1B*, *IL12p40*, *IFNB*, *iNOS*, *IL10*, *Fizz1* and *ArgI*) was normalized to the expression of Actin by the $2^{-\Delta\Delta CT}$ method.

Flow cytometry

WT and MGMT-KO BMMs were treated as described for each experiment. FC receptors were blocked with 10% serum and subsequently washed with FACS buffer before being stained with a mouse anti-mouse CD86 primary antibody or mouse anti-mouse CD40 primary antibody and then with an anti-mouse IgG (H + L) Alexa Fluor 488 secondary antibody (BioLegend), an anti-mouse MHC-II FITC antibody (BioLegend), and an anti-mouse CD206-PE antibody (BioLegend), all in the dark.

For measurement of the mean fluorescence intensity (MFI) of MitoTracker, macrophages in 6-well plates were incubated with MitoTracker Green FM (100 nM) (Thermo Fisher Scientific, USA) for 15 min. For bafilomycin A1 + Poly IC treatment, a 1-hr pretreatment with bafilomycin A1 (500 nM) (Sigma Aldrich, USA) was followed by a 24-hr treatment with Poly IC (20 μg/ml) before incubation with MitoTracker. Finally, the stained macrophages were subjected to analysis via flow cytometry. The acquired data were analyzed using FlowJo data analysis software (Tree Star, Inc., USA).

Sandwich ELISA

WT and MGMT-KO BMMs were prepared as described above. The medium in each well was replaced with 1000 μl of complete DMEM only (Unst.) or 1000 μl of complete DMEM with poly (I:C) (20 μg/ml) and incubated again for the indicated times. The culture supernatant was collected for each condition and preserved at -80 °C for use in ELISA. An ELISA MAX™ Standard Set (BioLegend, USA) for TNF-α or mouse IL-6 or IL-10 was used for sandwich ELISA. All reagents used for ELISA, unless otherwise specified, were obtained from BioLegend (USA) and were prepared according to the manufacturer's instructions.

Cytoplasmic and nuclear protein isolation

To investigate the cellular localization of MGMT, cytoplasmic protein was mildly extracted directly from BMMs on a tissue culture dish using a SimpleChIP® Enzymatic Cell Lysis Buffer A (Cell Signaling Technology, USA) and incubated on ice until cytoplasmic lysis was observed under the light microscope. The protein lysate was subsequently harvested by centrifugation at 12,000×*g* to fractionate the cytoplasmic protein and nuclei. The cytoplasmic protein lysate in the supernatant was collected into a new sterile tube, while the remaining pellet (nuclear fraction) was then extracted using high-salt RIPA buffer. The protein lysates were kept at − 80 °C until use.

Western blot

WT and MGMT KO BMMs were prepared, treated with poly (I:C) (20 μg/ml) and incubated for the indicated times. For bafilomycin A1 + poly (I:C) treatment, a 1-hr pretreatment with bafilomycin A1 (500 nM) (Sigma–Aldrich, USA) was followed by a 24-hr treatment with poly (I:C) (20 μg/ml). The cell lysates were collected at the indicated times using RIPA buffer (50 mM Tris HCl pH 7.4, 150 mM (for other proteins) or 500 mM (for histone) NaCl, 5 mM EDTA, 1% nonidet P-40, 0.5% sodium deoxycholate supplemented with protease and phosphate inhibitors (Cell Signaling Technology, USA)). The protein concentrations were measured via a bicinchoninic acid assay using the Pierce BCA Protein Assay Kit (Thermo-Fisher Scientific, USA). Proteins were separated via SDS–PAGE and subjected to Western blotting as described previously. The antibodies were diluted in PBS with 3% (w/v) skim milk at the following concentrations: rabbit anti-phospho-AMPK-α antibody, 1:1000; rabbit anti-total AMPK-α antibody, 1:1000; rabbit anti-phospho-mTOR antibody, 1:1000; rabbit anti-total mTOR antibody, 1:1000; rabbit anti-LC3B antibody, 1:1000; goat anti-rabbit IgG HRP, 1:4000; and goat anti-rat IgG HRP, 1:4000 (all from Cell Signaling Technology, USA); rat anti-MGMT antibody, 1:1000 (R&D system, USA); mouse anti-actin antibody, 1:10,000 (Merck Millipore, USA); and sheep anti-mouse IgG HRP, 1:4000 (GE Healthcare Life Sciences, USA). The signal was detected via the enhanced chemiluminescence (ECL) method. The relative intensity was analyzed via ImageJ analysis. Uncropped images of the Western blots are shown in Supplementary Fig. S10.

Fluorescence microscopy

WT and MGMT KO BMMs were seeded (3×10^5 cells/chamber/300 μl in BMM media) on chamber slides (Nunc™ Lab-Tek™ II Chamber Slide™ System; Thermo Fisher Scientific, USA) and incubated for 24 h. BMMs in each chamber were treated as indicated and subjected to staining. To stain acidic vacuoles such as autophagolysosomes in macrophages, the cells were incubated with fluorescence dye (LysoTracker™ Deep Red, Thermo Fisher Scientific, USA) for 1 h before fixation. To stain for mitochondrial superoxide, the macrophages were treated with MitoSOX reagent (5 μM) (Thermo Fisher Scientific, USA) for 10 min before fixation. For fixation, the medium was replaced with 1 ml of fixative (4% paraformaldehyde), and the mixture was incubated for 10 min at room temperature. The fixed cells were permeabilized with 1 mL of 0.1% Triton X-100/PBS for 3 min at room temperature. The cells were subsequently washed 3 times with 1X PBS (5 min each). After washing, the cells were blocked for 1 h at room temperature with blocking solution (3% BSA in 1X PBS). The cells were incubated with a rabbit anti-γ-H2AX antibody (Cell Signaling Technology, USA) at a dilution of 1:200, a rabbit anti-LC3B antibody (Cell Signaling Technology, USA) at a dilution of 1:200, a rabbit anti-MGMT antibody (Cell Signaling Technology, USA) at a dilution of 1:60, or a mouse anti-HSP60 antibody (DSHB, USA) at a concentration of 1 μg/mL in blocking solution at 4 °C overnight. The cells were washed 3 times (5 min each time) with 1X PBS the following day and incubated with an Alexa 488-conjugated anti-rabbit antibody (Cell Signaling Technology, USA), Alexa 488-conjugated anti-mouse antibody (Thermo Fisher Scientific, USA), Alexa 555-conjugated anti-rabbit antibody (Thermo Fisher Scientific, USA), or Alexa 405-conjugated anti-rabbit antibody (Thermo Fisher

Scientific, USA) at 1:500 in blocking solution at room temperature for 2 h. The cells were washed 3 times (5 min each time) with 1× PBS and stained with Hoechst for visualization of the nucleus. After washing with PBS, the slides were mounted with ProLong Gold Antifade Mountant (Life Technologies, USA), and the cells were analyzed via confocal laser scanning microscopy.

Fluorescence intensity measurement

WT and MGMT KO BMMs were cultured and treated as indicated above. For detection of MitoTracker Green fluorescence intensity in macrophages, macrophages in a 96-well black wall/clear bottom plate were incubated with MitoTracker Green (100 nM) for 15 min, followed by fixation with cold methanol and measurement of the fluorescence intensity of MitoTracker Green immediately at 490/516 nM with a multimode microplate reader (Ensight, PerkinElmer, USA). To detect the intensity of the ROS in the macrophages, the cells in the 96-well black wall/clear bottom plate were treated with DCFH-DA (10 μM) (Merck, USA) for 15 min, followed by washing with PBS, and the fluorescence intensity of the ROS was immediately measured at 498/520 nM with a multimode microplate reader.

ATP assay

WT and MGMT KO BMMs treated as indicated were lysed in 50 μL of Mammalian Cell Lysis Solution (MCLS), and the plates were shaken vigorously with an orbital shaker for 10 min. Fifty microliters of substrate solution (ATPLite; PerkinElmer) was added to each well and mixed vigorously (5–7 times) by pipetting. The plates were then incubated in the dark at room temperature for 15 min. After incubation, 50 μL of the sample was transferred from each well of a 96-well culture plate to the respective well of an OptiPlate-96. Finally, the OptiPlate-96 was sealed, and the luminescence was read under standard settings in a multimode microplate reader.

MTT assay

WT and MGMT KO BMMs were treated as indicated. After the incubation period, 10 μl of the MTT reagent (final concentration of 0.5 mg/ml) was added to each well, and the reactions were incubated for an additional 4 h. This step was followed by the addition of 500 μl of DMSO into each well and incubation for 2 h for complete solubilization of the purple formazan crystals. The absorbance of each sample was measured via a microplate reader at 540 nm.

Transcriptomic analysis

All RNA sequencing data were obtained as previously described[10] and can be found under the GEO accession number GSE231419. Subsequently, differential expressed genes (DEGs) in unstimulated WT and MGMT-KO BMM were compared and analyzed using the R package DESeq2 with a p-value cutoff of <0.05. DEGs that were either upregulated or downregulated significantly in MGMT KO macrophages were subjected to Gene Set Enrichment Analysis (GSEA) using GSEA software (GSEA 4.3.2). Gene set mh.all.v2023.1.Mm.symbols.gmt was used as gene set database for GSEA. Gene set was selected as permutation type and number of permutations was 1000. Mouse_Ensembl_Gene_ID_MSigDB.v2023.1.Mm.chip was used as Chip Platform. Significant GSEA pathways were selected with a p-value <0.05 and a false discovery rate (FDR) <0.05.

Statistical analysis

All experiments were performed in triplicate and at least three times independently. Statistical analyses were performed using GraphPad Prism version 5.0. Two-tailed unpaired t tests ($\alpha=0.05$) were used when comparing the two conditions. A P value of less than 0.05 was considered statistically significant. This study is reported in accordance with the ARRIVE guidelines.

Data availability

Data can be availed from the corresponding author, Tanapat Palaga (tanapat.p@chula.ac.th).The datasets generated analyzed during the current study are available under the GEO accession number GSE231419.

Received: 15 July 2024; Accepted: 5 November 2024
Published online: 11 November 2024

References

1. Christmann, M., Verbeek, B., Roos, W. P. & Kaina, B. O(6)-Methylguanine-DNA methyltransferase (MGMT) in normal tissues and tumors: enzyme activity, promoter methylation and immunohistochemistry. *Biochim. Biophys. Acta*. **1816**, 179–190. https://doi.org/10.1016/j.bbcan.2011.06.002 (2011).
2. Bai, P. et al. The dual role of DNA repair protein MGMT in cancer prevention and treatment. *DNA Repair. (Amst)*. **123**, 103449. https://doi.org/10.1016/j.dnarep.2023.103449 (2023).
3. Murawska, G. M. et al. Repurposing the Damage Repair Protein Methyl Guanine Methyl Transferase as a Ligand Inducible Fusion Degron. *ACS Chem. Biol.* **17**, 24–31. https://doi.org/10.1021/acschembio.1c00771 (2022).
4. Oldrini, B. et al. MGMT genomic rearrangements contribute to chemotherapy resistance in gliomas. *Nat. Commun.* **11**, 3883. https://doi.org/10.1038/s41467-020-17717-0 (2020).
5. Mantovani, A., Allavena, P., Marchesi, F. & Garlanda, C. Macrophages as tools and targets in cancer therapy. *Nat. Rev. Drug Discov.* **21**, 799–820. https://doi.org/10.1038/s41573-022-00520-5 (2022).
6. Kay, J., Thadhani, E., Samson, L. & Engelward, B. Inflammation-induced DNA damage, mutations and cancer. *DNA Repair. (Amst)*. **83**, 102673. https://doi.org/10.1016/j.dnarep.2019.102673 (2019).
7. Andersen, R. S., Anand, A., Harwood, D. S. L. & Kristensen, B. W. Tumor-Associated Microglia and macrophages in the Glioblastoma Microenvironment and their implications for Therapy. *Cancers (Basel)*. 13. https://doi.org/10.3390/cancers13174255 (2021).

8. Geiger-Maor, A. et al. Macrophages regulate the systemic response to DNA damage by a cell nonautonomous mechanism. *Cancer Res.* **75**, 2663–2673. https://doi.org/10.1158/0008-5472.CAN-14-3635 (2015).
9. Benjaskulluecha, S. et al. Screening of compounds to identify novel epigenetic regulatory factors that affect innate immune memory in macrophages. *Sci. Rep.* **12**, 1912. https://doi.org/10.1038/s41598-022-05929-x (2022).
10. Benjaskulluecha, S. et al. O(6)-methylguanine DNA methyltransferase regulates beta-glucan-induced trained immunity of macrophages via farnesoid X receptor and AMPK. *iScience* **27**, 108733. https://doi.org/10.1016/j.isci.2023.108733 (2024).
11. Lind, N. A., Rael, V. E., Pestal, K., Liu, B. & Barton, G. M. Regulation of the nucleic acid-sensing toll-like receptors. *Nat. Rev. Immunol.* **22**, 224–235. https://doi.org/10.1038/s41577-021-00577-0 (2022).
12. Yang, Q. & Shu, H. B. Deciphering the pathways to antiviral innate immunity and inflammation. *Adv. Immunol.* **145**, 1–36. https://doi.org/10.1016/bs.ai.2019.11.001 (2020).
13. Nikolova, T. et al. The gammaH2AX assay for genotoxic and nongenotoxic agents: comparison of H2AX phosphorylation with cell death response. *Toxicol. Sci.* **140**, 103–117. https://doi.org/10.1093/toxsci/kfu066 (2014).
14. Cai, S. et al. Mitochondrial targeting of human O6-methylguanine DNA methyltransferase protects against cell killing by chemotherapeutic alkylating agents. *Cancer Res.* **65**, 3319–3327. https://doi.org/10.1158/0008-5472.CAN-04-3335 (2005).
15. Wang, Y., Li, N., Zhang, X. & Horng, T. Mitochondrial metabolism regulates macrophage biology. *J. Biol. Chem.* **297**, 100904. https://doi.org/10.1016/j.jbc.2021.100904 (2021).
16. Bhatia, V. & Sharma, S. Role of mitochondrial dysfunction, oxidative stress and autophagy in progression of Alzheimer's disease. *J. Neurol. Sci.* **421**, 117253. https://doi.org/10.1016/j.jns.2020.117253 (2021).
17. Redza-Dutordoir, M. & Averill-Bates, D. A. Interactions between reactive oxygen species and autophagy: special issue: death mechanisms in cellular homeostasis. *Biochim. Biophys. Acta Mol. Cell. Res.* **1868**, 119041. https://doi.org/10.1016/j.bbamcr.2021.119041 (2021).
18. Yun, H. R. et al. Roles of autophagy in oxidative stress. *Int. J. Mol. Sci.* **21** https://doi.org/10.3390/ijms21093289 (2020).
19. Canton, M. et al. Reactive oxygen species in macrophages: sources and targets. *Front. Immunol.* **12**, 734229. https://doi.org/10.3389/fimmu.2021.734229 (2021).
20. Hinchy, E. C. et al. Mitochondria-derived ROS activate AMP-activated protein kinase (AMPK) indirectly. *J. Biol. Chem.* **293**, 17208–17217. https://doi.org/10.1074/jbc.RA118.002579 (2018).
21. Lee, E., Choi, J. & Lee, H. S. Palmitate induces mitochondrial superoxide generation and activates AMPK in podocytes. *J. Cell. Physiol.* **232**, 3209–3217. https://doi.org/10.1002/jcp.25867 (2017).
22. Liu, R. et al. Spermidine endows macrophages anti-inflammatory properties by inducing mitochondrial superoxide-dependent AMPK activation, Hif-1alpha upregulation and autophagy. *Free Radic Biol. Med.* **161**, 339–350. https://doi.org/10.1016/j.freeradbiomed.2020.10.029 (2020).
23. Li, M. Y. et al. Adrenomedullin alleviates the pyroptosis of Leydig cells by promoting autophagy via the ROS-AMPK-mTOR axis. *Cell. Death Dis.* **10**, 489. https://doi.org/10.1038/s41419-019-1728-5 (2019).
24. Onishi, M., Yamano, K., Sato, M., Matsuda, N. & Okamoto, K. Molecular mechanisms and physiological functions of mitophagy. *EMBO J.* **40**, e104705. https://doi.org/10.15252/embj.2020104705 (2021).
25. Ma, K. et al. Mitochondrial homeostasis, and cell fate. *Front. Cell. Dev. Biol.* **8**, 467. https://doi.org/10.3389/fcell.2020.00467 (2020). Mitophagy.
26. Mauvezin, C. & Neufeld, T. P. Bafilomycin A1 disrupts autophagic flux by inhibiting both V-ATPase-dependent acidification and Ca-P60A/SERCA-dependent autophagosome-lysosome fusion. *Autophagy*. **11**, 1437–1438. https://doi.org/10.1080/15548627.2015.1066957 (2015).
27. Lieber, M. R. The mechanism of double-strand DNA break repair by the nonhomologous DNA end-joining pathway. *Annu. Rev. Biochem.* **79**, 181–211 (2010).
28. Vier, J., Häcker, G. & Kirschnek, S. Contribution of A1 to macrophage survival in cooperation with MCL-1 and BCL-XL in a murine cell model of myeloid differentiation. *Cell Death Dis.* **15**, 677 (2024).
29. Robles, S. J. & Adami, G. R. Agents that cause DNA double strand breaks lead to p16INK4a enrichment and the premature senescence of normal fibroblasts. *Oncogene*. **16**, 1113–1123. https://doi.org/10.1038/sj.onc.1201862 (1998).
30. Harberts, E. & Gaspari, A. A. TLR signaling and DNA repair: are they associated? *J. Invest. Dermatol.* **133**, 296–302. https://doi.org/10.1038/jid.2012.288 (2013).
31. Sallmyr, A., Fan, J. & Rassool, F. V. Genomic instability in myeloid malignancies: increased reactive oxygen species (ROS), DNA double strand breaks (DSBs) and error-prone repair. *Cancer Lett.* **270**, 1–9. https://doi.org/10.1016/j.canlet.2008.03.036 (2008).
32. Nowosielska, A. & Marinus, M. G. DNA mismatch repair-induced double-strand breaks. *DNA Repair. (Amst)*. **7**, 48–56. https://doi.org/10.1016/j.dnarep.2007.07.015 (2008).
33. Casorelli, I., Russo, M. T. & Bignami, M. Role of mismatch repair and MGMT in response to anticancer therapies. *Anticancer Agents Med. Chem.* **8**, 368–380. https://doi.org/10.2174/187152008784220276 (2008).
34. Chen, Y., Lin, J., Zhao, Y., Ma, X. & Yi, H. Toll-like receptor 3 (TLR3) regulation mechanisms and roles in antiviral innate immune responses. *J. Zhejiang Univ. Sci. B.* **22**, 609–632. https://doi.org/10.1631/jzus.B2000808 (2021).
35. Kawasaki, T. & Kawai, T. Toll-like receptor signaling pathways. *Front. Immunol.* **5**, 461. https://doi.org/10.3389/fimmu.2014.00461 (2014).
36. Reimer, T., Brcic, M., Schweizer, M. & Jungi, T. W. Poly(I:C) and LPS induce distinct IRF3 and NF-kappaB signaling during type-I IFN and TNF responses in human macrophages. *J. Leukoc. Biol.* **83**, 1249–1257. https://doi.org/10.1189/jlb.0607412 (2008).
37. Kim, K. S. et al. Frontline Science: estrogen-related receptor gamma increases poly(I:C)-mediated type I IFN expression in mouse macrophages. *J. Leukoc. Biol.* **109**, 865–875. https://doi.org/10.1002/JLB.2HI1219-762R (2021).
38. De Miranda, J., Yaddanapudi, K., Hornig, M. & Lipkin, W. I. Astrocytes recognize intracellular polyinosinic-polycytidylic acid via MDA-5. *FASEB J.* **23**, 1064–1071. https://doi.org/10.1096/fj.08-121434 (2009).
39. Rong, Z. et al. The mitochondrial response to DNA damage. *Front. Cell. Dev. Biol.* **9**, 669379. https://doi.org/10.3389/fcell.2021.669379 (2021).
40. Hahn, A. & Zuryn, S. Mitochondrial genome (mtDNA) mutations that generate reactive oxygen species. *Antioxid. (Basel)*. **8** https://doi.org/10.3390/antiox8090392 (2019).
41. Zhang, Y. et al. Spinetoram confers its cytotoxic effects by inducing AMPK/mTOR-mediated autophagy and oxidative DNA damage. *Ecotoxicol. Environ. Saf.* **183**, 109480. https://doi.org/10.1016/j.ecoenv.2019.109480 (2019).
42. Martín-Jiménez, R., Lurette, O. & Hebert-Chatelain, E. Damage in mitochondrial DNA associated with Parkinson's Disease. *DNA Cell Biol.* **39**, 1421–1430 (2020).
43. Hahn, A. & Zuryn, S. Mitochondrial genome (mtDNA) mutations that generate reactive oxygen species. *Antioxidants.* **8**, 392 (2019).
44. Wu, K. K. L. et al. The APPL1-Rab5 axis restricts NLRP3 inflammasome activation through early endosomal-dependent mitophagy in macrophages. *Nat. Commun.* **12**, 6637 (2021).
45. Bhatia, D. et al. Mitophagy-dependent macrophage reprogramming protects against kidney fibrosis. *JCI Insight* 4 (2019).

Acknowledgements

This research has received funding support from the NSRF via the Program Management Unit for Human Resources & Institutional Development, Research and Innovation (grant number B16F640117) and by Thailand

Science Research and Innovation Fund Chulalongkorn University (FF67). AL is supported by the Program Management Unit for Human Resources & Institutional Development, Research and Innovation (grant number B16F640175). This work was partly conducted by the joint research program of the Research Center for GLOBAL and LOCAL Infectious Diseases, Oita University (2023B12). FH and AB are supported by the Second Century Fund (C2F), Chulalongkorn University. This study was partially supported by the NSRF via the Program Management Unit for Human Resources & Institutional Development, Research Innovation (Grant No. B13F670075). PKV is supported by the Ratchadapisek Somphot Fund for Postdoctoral Fellowship, Chulalongkorn University.

Author contributions

FH designed and performed all experiments, analyzed all data and prepared all figures and drafted the manuscripts. SB prepared mice and cells. AB and PKV supported animal colony maintenance. BW, TPK, RO, KS, CP performed ELISA, PCR, and Western blot and analyzed the data in some experiments. BS performed animal genotyping. PKJ analyzed RNA sequencing data. TK and AL advised on experimental designs and acquired grant funding. TPG supervised the overall project, acquired grant fundings, designed all experiments, analyzed data, and prepared the manuscript.

Declarations

Competing interests

The authors declare no competing interests.

Additional information

Supplementary Information The online version contains supplementary material available at https://doi.org/10.1038/s41598-024-78885-3.

Correspondence and requests for materials should be addressed to T.P.

Reprints and permissions information is available at www.nature.com/reprints.

Publisher's note Springer Nature remains neutral with regard to jurisdictional claims in published maps and institutional affiliations.